14th Australasian Fluid Mechanics Conference
Adelaide University, Adelaide, Australia
10-14 December 2001

Sound emission processes on bubble detachment

R.Manasseh[1], A.Bui[1], J.Sandercock[2], A.Ooi[2]

[1]CSIRO Thermal & Fluids Engineering
PO Box 56, Highett, VIC 3190, Melbourne, AUSTRALIA

[2]Department of Mechanical Engineering
University of Melbourne, Parkville, VIC 3010, Melbourne, AUSTRALIA

Abstract

Experimental and numerical studies were conducted on the first few milliseconds of a bubble's sound emission.

Bubbles can oscillate volumetrically, emitting sound at a frequency characteristic of their radius and ambient pressure. This well-known phenomenon is responsible for much of the audible noise generated by liquids in motion. It has applications in bubbly-flow analysis software which is useful in food and minerals processing, biotechnology, medicine and oceanography. Understanding of the detailed processes causing bubble sound emission could yield more efficient sound-processing algorithms.

Acoustic signals from continuously-sparged laboratory bubbles were fed through a variable-delay trigger, acquiring high-resolution optical images at any desired phase of the bubble formation. Numerical simulations were performed by a compressible Navier-Stokes solver using a level-set interface-tracking method. Thus, each stage of the sound-emission process could be compared with data from numerical calculations.

Experiments revealed that the initial drop in the acoustic signal was co-incident with the contraction of the bubble neck during the detachment process. The acoustic signal peak co-incided with a jet of liquid penetrating the bubble after neck breaking. In a first step towards explaining these observations, the compressible numerical model reproduced the theoretical oscillation frequency as well as the initial drop and subsequent peak on bubble detachment.

Introduction

The emission of an acoustic signal by bubbles on formation and deformation is well known [5, 8, 11]. A full review of bubble acoustics is given by Leighton [6]. The fundamental relation between bubble acoustic frequency, ambient pressure and radius was found by Minnaert [11]. Equating the potential energy of the compressed gas with the kinetic energy of the fluid set in motion around the bubble gives

$$2\pi f_0 = \sqrt{\frac{3\gamma P_0}{\rho}}\,\frac{1}{R_0}, \qquad (1)$$

where f_0 is the frequency in Hz, P_0 is the absolute liquid pressure, γ is the ratio of specific heats for the gas, ρ is the liquid density, and R_0 is the bubble radius. It can be shown that surface tension is a second-order effect [8], so it is usually neglected except for microscopic bubbles. Rather than assuming a linear harmonic oscillation, a more general history of the bubble oscillation may be obtained by solving the Rayleigh-Plesset equation, a one-dimensional ordinary differential equation for R_0 [12]. However, the initial pressure perturbation must first be known, and for bubbles being formed the initial pressure history is presently unknown.

Bubble sounds in environmental systems like the ocean have been used to calculate bubble size spectra (e.g. Leighton & Walton [5]). Chemical engineering applications of passive acoustic bubble sizing were reviewed by Boyd & Varley [1]. In addition to minerals processing and chemical and polymer manufacture, controlled bubbling of gas into liquid is an essential part of genetic-engineering reactors, fermentation, and wastewater treatment. In metallurgy, the size of bubbles in liquid metals affects mass and heat transfer, as well as the porosity of the product. In medicine, bubbles in blood are a contaminant that must be detected.

In industrial aerators, large (2-4 mm radius) bubbles are typically sparged rapidly from a nozzle. Manasseh [9] found that under these conditions the acoustic frequency was not a constant and varied during the pulse, implying that the assumption of linear oscillation inherent in (1) is not valid in practical cases. Significant errors are introduced if a simplistic approach, like Fourier transforming the whole pulse, is used to determine the bubble size. This raises the question of what is the most correct form of measurement to make, and what the various stages of the acoustic signal correspond to physically.

As a bubble is pinched off, its neck retracts abruptly. This causes a radial inrush of liquid that penetrates the bubble, forming a jet [10]. It is possible that this jet compresses the gas within the bubble, priming the acoustic oscillation. An alternative explanation for sound generation is a nonlinear process that transfers energy from shape distortions [7]. To assess these sound-generation theories, the sound emission in the first few milliseconds of a bubble's life should be examined. A necessary first step is to see if a compressible Navier-Stokes solver can reproduce an experimentally-observed oscillatory pressure trace; this is the focus of the present paper.

Methods

Experimental Method

Air bubbles were produced from an underwater nozzle with internal diameter 6.0 mm. The nozzle was machined to maintain its internal edge as sharp as possible, which ensured a known contact radius for the forming bubble. The bubbles were produced from compressed and filtered air in pressure-controlled mode [4]. The liquid was water and the nozzle orifice was at a depth of 0.23 m. A hydrophone (Bruel & Kjaer 8103) with a linear response in the bubble frequency range was placed about 15 mm away from the bubble neck-break point.

The technique used here relies on the high degree of repeatability of bubble formation and is detailed in [10]. A photograph at any desired phase of the acoustic pulse

was triggered from the acoustic signal itself. The resulting series of images achieves higher temporal resolution than the best gained by motion-picture techniques [14].

Numerical Simulation Method

Manasseh et al.[10] used a Volume-Of-Fluid method for numerical simulations. This code was incompressible and thus unable to simulate the acoustic pressure signature. In the present work, an advanced modelling approach based on Eulerian representation of the flow field coupled with explicit interface tracking was used to simulate the bubble dynamics [2]. A front-capturing algorithm, named the Level Set Method, was applied to accurately follow the interfacial evolution in time. A high-order numerical scheme, called CIP (Cubic-Interpolated-Propagation) [15, 16], was utilized to solve the Navier-Stokes equation and the level-set equations with high accuracy and, at the same time, without the need for a stencil extension. The surface tension force is modelled and included as a source term in the momentum equations.

This method was developed by Yabe et al.[15] and has been successfully applied to solve the system of Navier-Stokes equations for both compressible and incompressible fluid flows [16]. In general, the CIP method *explicitly* solves the general convective-diffusion differential equations in two (non-advection and advection) phases. The CIP numerical scheme appears to be very accurate and effective in solving the level equation in comparison to other high-order schemes.

In addition to the high-order Navier-Stokes solver, a technique based on the front-capturing Level Set Algorithm (LSA) is also employed to ensure a sharp representation of the interface in time. The interface is described by the zero level of a smooth function, ϕ, which is convected by the flow field following

$$\phi_t + (\mathbf{u} \cdot \nabla)\phi = 0. \qquad (2)$$

This equation will move the zero level of ϕ on the Eulerian grid exactly as the actual interface moves. Since ϕ is a smooth function, unlike the field properties, (2) is easily solved numerically.

The level function, ϕ, can be initialized as a signed distance function, i.e.

$$\phi(\mathbf{x}, t = 0) = \pm d, \qquad (3)$$

where d is the distance from $\mathbf{x}$ to the interface, and the plus (minus) sign is chosen if the point $\mathbf{x}$ is outside (inside) the region bounded by the initial interface.

When solving the Navier-Stokes equations, in order to smooth the sharp property changes at the interface and to mitigate numerical oscillations, the properties are defined from the level-sets using a regularization Heaviside function.

The numerical discretization of the level set formulation does not preserve the total mass in time [3]. Therefore, simulation of a long transient problem may cause some mass loss. In order to overcome this problem, a re-initialization procedure was proposed [3, 13]. In [13], an iterative procedure re-initialized the level-set function at each time step, which helps to keep the re-initialized level-set function as a signed distance function. This re-initialization procedure can help to conserve the mass during transient simulations.

Results

Experimental Results

The system was set to produce bubbles at a rate of 13.57 ± 0.05 Hz. The repeatable regime of bubble formation, for the 6.0 mm nozzle under water 0.23 m deep, ranges from about 0.3 to 22 Hz. Figure 1 shows the acoustic signal produced by these bubbles on formation. It was band-pass filtered between 200 Hz and 3 kHz. This trace is perfectly repeatable over the first two cycles. Some variations in the signal amplitude occur in the third and fifth cycles. However, significant variations in bubble behaviour can only be visually discerned much later, after some tens of milliseconds. Figure 2 shows photographs of the bubble detachment.

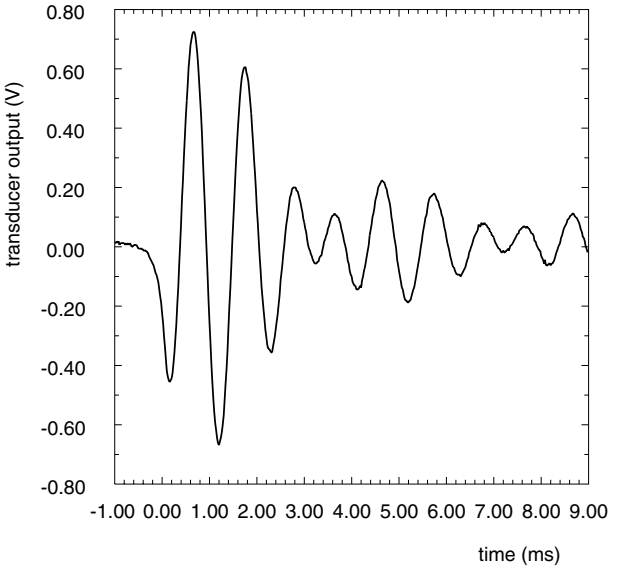

Figure 1: *Acoustic signal of a single bubble produced from a 6 mm nozzle. Bubbling rate* 13.57 ± 0.05 *Hz. Time* $t = 0$ *is at the instant of bubble detachment.*

The acoustic frequency is 0.950 ± 0.002 kHz, measured from the first period of oscillation (first trough to second trough; 1.053 ms). This measurement was shown [9] to be the most accurate way of determining bubble radius using (1). The first 2 ms of the signal is shown in figure 3. If bubbles are produced more rapidly, or there is more viscous or thermal dissipation, only the first period may be present.

In figure 3 the dashed lines show the times of the series of six photographs in figure 2. Time $t = 0$ has been set to the time of figure 2(b), which was taken as close as practical to the actual neck-breaking event. The times have been adjusted for the signal delay time. Thus the values marked 'a–f' on the curve are proportional to the true pressure in the vicinity of the neck-breaking point, at the instant the flash which created the corresponding image reached maximum intensity. The interval between *(a)* and *(b)* is 100 ± 4 μs while the intervals between *(b)*, *(c)* and *(d)* are 33 ± 4 μs. There is little change in the shape of the attached bubble or its neck in the 200 μs or so prior to *(a)*, but dramatic change in the subsequent 170 μs as the neck breaks.

It can be seen that the neck-breaking process occurs as the acoustic signal pressure is falling. The initial fall of the signal to its first minimum, which is always noticed

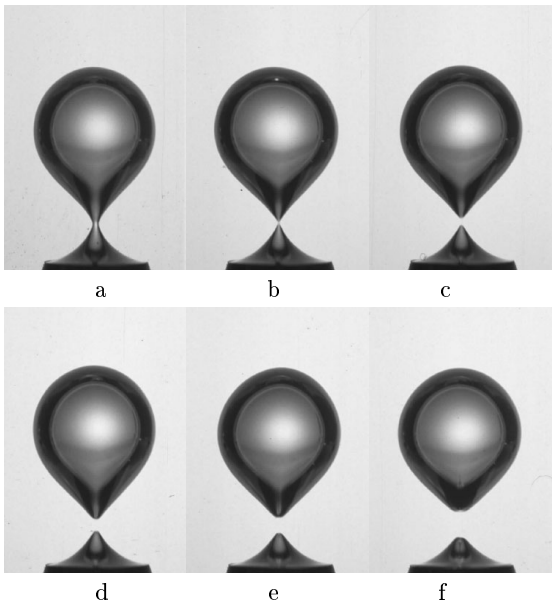

Figure 2: *Photographs of neck-breaking phase of bubble detachment and beginning of jet formation. Note nozzle orifice at picture bottom is 6 mm across. Corresponding acoustic signal shown in figure 3.*

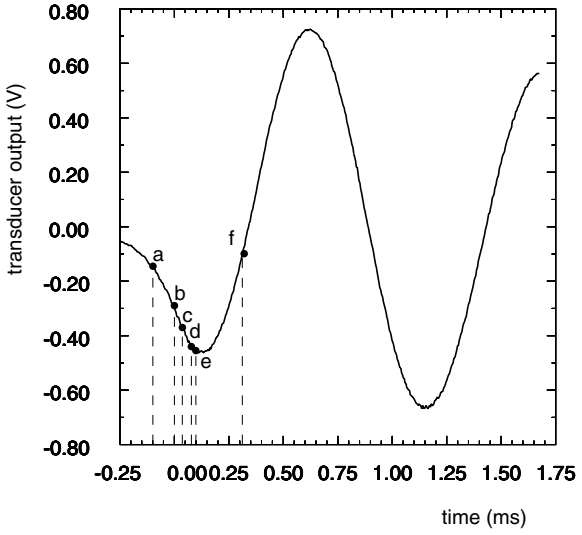

Figure 3: *Detail of the acoustic signal of figure 1. Labels a - f correspond to the photographs in figure 2*

as a bubble detaches, corresponds to the broken tip of the neck retracting. In [10], the tip of the neck was estimated to be retracting into the bubble at roughly 5 m s^{-1}.

There is an interesting difference between the images of figure 2*(e)* and *(f)*. In *(e)*, the retracting tip of the bubble is still convex in form; light passes through the tip, accounting for the bright streak along the centreline of the tip – just as in the earlier images of figure 2. However, in *(f)*, this bright streak has disappeared. In its place is a thin dark line that corresponds to a jet of liquid penetrating the bubble [10]. The photograph (not reproduced here) taken between the times of *(e)* and *(f)* and 100μs after *(e)* looks very similar to *(e)*. Thus, the jet has formed during the 100μs prior to *(f)*. As noted above, the jet is due to a radial inrush of liquid.

Numerical Simulation Results

A two-dimensional Cartesian version of the numerical code was used. Although an axisymmetric formulation would be preferable, at the time of writing instabilities associated with singularites on the axis were preventing use of the axisymmetric version. The physics of the 2D-Cartesian simulation should not be expected to match that of an axisymmetric simulation, nor the three-dimensional experiment. In particular, in a 2D-Cartesian simulation the simple inverse relationship (1) between f_0 and R_0 is not valid. The 2D-Cartesian equivalent of (1), calculated like (1) by equating maximal potential and kinetic energies, is

$$2\pi f_0 = \sqrt{\frac{2\gamma P_0}{\rho}}\,\frac{1}{R_0\sqrt{\ln\left(D/R_0\right)}}, \qquad (4)$$

where D is a measure of the finite domain size. As $D \to R_0$, $f_0 \to \infty$, introducing instabilities; stability was found for a physical domain size greater than or equal to 0.02176×0.02176 m, corresponding to $D/R_0 \sim 7$. Although the frequency-radius relation is domain-size dependent in a 2D-Cartesian system, the relationship

$$f_0 \propto \sqrt{P_0}, \qquad (5)$$

is still valid and could be regarded as a basic test of the code's ability to reproduce the effect of compressibility. A bubble density of 80 kg m^{-3} and viscosity 0.001 Pa s was used. The liquid density and viscosity had their usual physical values of 1000 kg m^{-3} and 0.001 Pa s. A test of (5) was made by varying P_0 in a 64×64 grid in a domain of physical size 0.02176×0.02176 m. Other parameters were chosen to match the experiment. The initial bubble shape was a sphere attached to a cylinder modelling the parent body of gas in the nozzle.

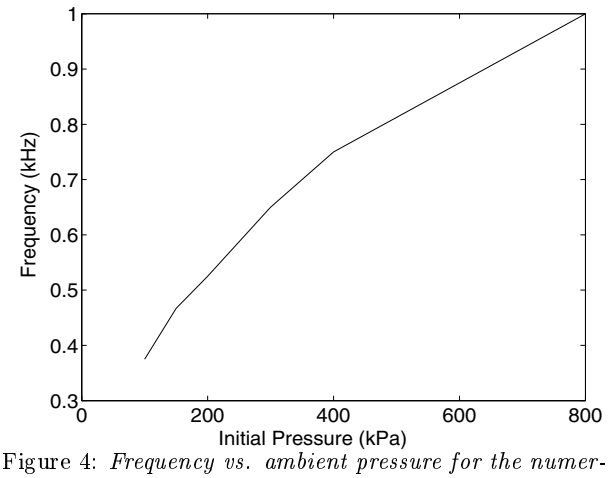

Figure 4: *Frequency vs. ambient pressure for the numerical simulation.*

After initialization the discontinuity between the cylinder and sphere caused an immediate relaxation in bubble shape. This process created oscillations in the pressure. To compare the oscillation frequency with a theory, the numerical bubble and its three impermeable domain boundaries were modelled by a set of six potential-flow sources, yielding the kinetic energy needed to calculate a frequency in the same manner as (1) or (4). For P_0 = 100 kPa, theory predicts $f_0 \simeq$ 400 Hz, in good agreement with the simulated oscillation frequency. Moreover, it can be seen in figure 4 that the trend in f_0

with P_0 agrees with (5). The oscillations could be eliminated by making the gas incompressible (by increasing γ by four orders of magnitude) confirming the oscillations are indeed due to compressibility.

As the bubble forms a neck and begins to break off, the pressure history (figure 5) again shows an oscillation. Here the physical domain size was 0.04352×0.04352 m. There is an initial dip in pressure and a subsequent rise to a peak, similarly to the experimental pressure history (figure 3). The approximate frequency of this first period is about 290 Hz; the potential-flow theory predicts about 330 Hz. However, the sequence of events is shifted in time; in the simulation the neck-breaking event occurred after the peak in acoustic signal pressure, while in the experiment it occurred during the initial dip. It is not certain if this is due to the different physics of the 2D-Cartesian calculation or another artefact of the simulation.

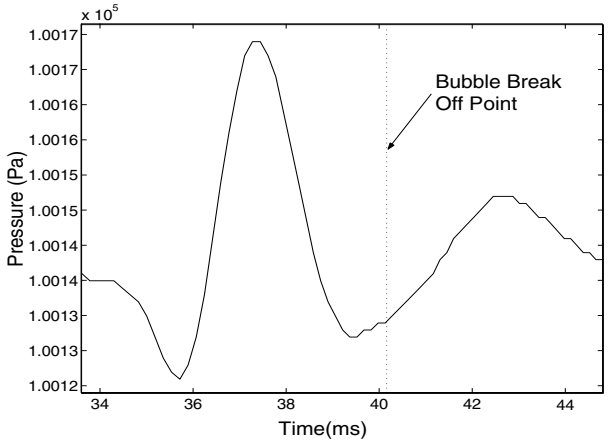

Figure 5: *Pressure vs. Time for the numerical simulation as measured at the point (13.6mm, -13.6mm).*

Conclusions

A simple 2D compressible model successfully reproduced the theoretical acoustic oscillation frequency of a bubble on its formation from a parent body of gas.

Experiments found that an initial drop in pressure is associated with the neck-breaking process and the rapid retraction of the tip of the bubble once it has detached. It was hypothesized that the subsequent penetration of the bubble by a jet compressed the gas in the bubble, priming the oscillation. Details of the oscillation during the neck-breaking process were also successfully simulated, although the sequence of geometric and pressure histories differs from the experiment.

Future work is expected to develop the model for an axisymmetric simulation. If the initial pressure history on bubble breakoff can be successfully parameterized, a simple quasi-analytic model of the subsequent oscillation based on the Rayleigh-Plesset equation should be feasible.

Acknowledgements

We are grateful to Tony Swallow and Tony Antzakas, who designed and built the trigger-delay circuit.

References

[1] Boyd, J. W. R., Varley, J., The Uses of Passive Measurement of Acoustic Emissions from Chemical Engineering Processes, *Chem. Eng. Sci.*, **56**, 2001, 1749–1767

[2] Bui, A., Dinh, T. N., Sehgal, B. R., Numerical Simulation of Interface Phenomena using CIP and the Level Set Front-Capturing Method, *Comp. Fluid Dynamics*, **8**(1), 1999, 103–112

[3] Y.C. Chang, T.Y. Hou, B. Merriman, and S. Osher, A Level Set Formulation of Eulerian Interface Capturing Methods for Incompressible Fluid Flows, *J. Comp. Physics*, **124**, 1996, 449–464.

[4] Chhabra, R. P., *Bubbles, Drops, and Particles in non-Newtonian Flows,* CRC Press, Boca Raton, Florida, USA, 1993.

[5] Leighton, T. G., and Walton, A. J., An Experimental Study of the Sound Emitted by Gas Bubbles in a Liquid, *Eur. J. Phys.*, **8**, 1987, 98–104.

[6] Leighton, T. G., *The Acoustic Bubble,* Academic Press, London, 1994.

[7] Longuet-Higgins, M. S., Monopole Emission of Sound by Asymmetric Bubble Oscillations, Part 1: Normal Modes, *J. Fluid Mech.*, **201**, 1989, 525–541.

[8] Longuet-Higgins, M. S., Kerman, B. R., and Lunde, K., The Release of Air Bubbles from an Underwater Nozzle, *J. Fluid Mech.*, **230**, 1991, 365–390.

[9] Manasseh, R., LaFontaine, R. F., Davy, J., Shepherd, I. C. & Zhu, Y., Passive Acoustic Bubble Sizing in Sparged Systems. *Exp. Fluids*, **30** (6), 672–682.

[10] Manasseh, R., Yoshida, S., Rudman, M., Bubble Formation Processes and Bubble Acoustic Signals, *Third International Conference on Multiphase Flow, ICMF'98, Lyon, France, 8–12 June 1998*, 1998

[11] Minnaert, M., On Musical Air Bubbles and the Sound of Running Water, *Phil. Mag.*, **16**, 1933, 235–248.

[12] Plesset, M. S., The Dynamics of Cavitation Bubbles. *J. Appl. Mech.*, **16**, 1949, 277–282.

[13] Sussman, M., Smereka, P., Osher,S., A Level Set Approach for Computing Solutions to Incompressible Two-Phase Flow, *J. Comp. Physics*, **114**, 1994, 146–159.

[14] Tassin, A. L., Nikitopoulos, D. E., Non-Intrusive Measurements of Bubble Size and Velocity, *Exp. in Fluids*, **19**, 1995, 121–132.

[15] Yabe, T., Ishikawa, T., Kadota, Y., Ikeda, F., A Multidimensional Cubic-Interpolated Pseudoparticle (CIP) Method without Time Splitting Technique for Hyperbolic Equations, *J. Phys. Soc. Jpn*, **59**, 1990, 2301–2304.

[16] T. Yabe and P.Y. Wang, Unified Numerical Procedure for Compressible and Incompressible Fluid, *J. Phys. Soc. Jpn*, **60**, 1991, 2105–2108.